Journal of the European Ceramic Society 19 (1999) 2917–2930

PII: S0955-2219(99)00062-X
0955-2219/99/$ - see front matter

Fabrication of PMN and PFN Ceramics by a Two-Stage Sintering Technique

Supon Ananta and Noel W. Thomas*

Department of Materials, University of Leeds, Leeds LS2 9JT, UK

(Received 4 February 1999; accepted 28 February 1999)

Abstract

Relaxor perovskite ceramics of lead magnesium niobate (PMN) and lead iron niobate (PFN) have been prepared by employing a two-step mixed oxide synthetic route, followed by the application of a two-stage sintering method. The effect of the latter on phase formation, densification behaviour, microstructure and dielectric properties of both relaxor systems is examined. Two types of pyrochlore phase are found to co-exist with the major phase in the PMN system, i.e. $Pb_3Nb_4O_{13}$ and $Pb_{1.83}Nb_{1.71}Mg_{0.29}O_{6.39}$ with an MgO inclusion. By comparison, a $PbFe_8O_{13}$ pyrochlore phase with an Fe_2O_3 inclusion is observed in the PFN system. The types and concentrations of phases present are found to depend upon sintering conditions. In connection with dielectric properties, a substantial dependence of the maximum values of both relative permittivity ($\varepsilon'_{r,max}$) and dissipation factor ($\tan\delta_{max}$) on sintering regime is observed. By employing optimised two-stage sintering conditions, high density ceramics with low firing temperatures and reasonable relative permittivities can be achieved in both systems. © *1999 Elsevier Science Ltd. All rights reserved*

Keywords: sintering, dielectric properties, lead magnesium niobate, lead iron niobate, perovskites.

1 Introduction

In general, the overriding aim of any materials processing technique is to achieve a final product with consistent properties. In practice, the level of consistency obtained is often a matter of compromise, it being largely a consequence of the economics of fabrication and characterisation. The mixed oxide synthetic route is probably one of the most fundamental, practical routine methods which has been used, and it has been developed and modified in both scientific research and industrial mass production for many years.[1–11] This technique involves powder preparation (mixing, milling, drying, sieving and calcination), the forming of a green body and densification, where heat is applied, either with pressure (HIP) or without (sintering). Although many alternative synthetic routes such as co-precipitation, molten salt, sol–gel or hydrothermal methods have been introduced from time to time,[6,14] widespread efforts have still been made on the modification and development of conventional mixed oxide methods.[21–31]

Lead-based complex perovskites with the general formula A(B'B'')O_3, such as Pb($Mg_{1/3}Nb_{2/3}$)O_3; (PMN), Pb($Fe_{1/2}Nb_{1/2}$)O_3; (PFN), Pb($Zn_{1/3}Nb_{2/3}$)O_3; (PZN) and Pb($Fe_{2/3}W_{13}$)O_3; (PFW) have received considerable attention since the late 1970s and have been applied recently in areas such as multilayer ceramic capacitors (MLCCs) and electrostrictive actuators.[1–12] In connection with these applications, the ideal material would provide a high relative permittivity over the operational temperature range, together with a low dielectric loss. It would also be highly desirable for this material to be fired at relatively low temperatures, permitting the use of cheaper electrode materials such as nickel, copper or silver.[1–5] However, a practical limitation to the utilisation of these materials in device applications has been the lack of a simple, reproducible fabrication technique for a pure perovskite phase with consistent properties. The main hindrance to the commercial exploitation of lead-based complex perovskites arises from processing difficulties, concerned with the high volatility of lead oxide and the formation of pyrochlore phases.[11–20]

Several efforts[21–31] have been made to enhance processing techniques to create or develop materials

* To whom correspondence should be addressed at present address: WBB Technology Ltd., Watts Blake Bearne & Co plc, Park House, Courtenay Park, Newton Abbot TQ12 4PS, UK. Fax: +44-(0)1626-322-386; e-mail address: nthomas@wbb.co.uk

with properties approaching applicational requirements. These include (a) use of a two stage calcination route;[21,22,27] (b) using higher purity and finer, more reactive precursor powders;[11,24,26] (c) employing additives[15,16,28–31] and (d) carrying out repeated calcination and milling cycles.[23–26,34,35] These techniques affect the phase formation, structure and dielectric properties of materials in different ways. Amongst all the issues reported so far, most attention has been concentrated on the powder processing stage, whereas investigations of modified sintering techniques have not been widely carried out.

Two alternative techniques employing longer heat treatment, whilst reducing the firing temperature, were reported by Fu and Chen[34] for PFN powders and by Lejeune and Boilot[35] for PMN ceramics. The repeated calcination stage employed in the former work, corresponding to the so-called double calcination technique, demonstrated the possibility of obtaining single-phase PFN powder. The latter work, by comparison, paid attention to three sintering cycles (either 1000°C for 6 h or heating to 800/830°C followed by cooling down and heating to 1000°C again for 6 h. The second sintering cycle (i.e. heating to 800°C) was found to produce PMN ceramic with the best dielectric properties. Thus sintering is a crucial stage which can influence the dielectric properties of the final product more strongly than the choice of reaction precursors. This is because pyrochlore formation and lead volatilisation can easily become the predominant considerations for lead-based complex perovskite materials.

In the present study, an attempt has been made to fabricate and investigate the relaxor perovskites PMN and PFN by employing an alternative sintering method corresponding to the so-called double sintering technique. Instead of using a single, high firing temperature (of up to 1275 and 1175°C for PMN[32] and PFN,[33] respectively) or a long time of up to 6 h[35], two moderate temperatures (T_1 and T_2, with a constant dwell-time of 2 h at each stage) were adopted. In so doing, the effect of sintering conditions (T_1 and T_2) on phase formation, microstructure and dielectric properties of materials is monitored, paying attention to differences between the PMN and PFN systems. The motivation for carrying out this work is two-fold. First, the investigation and development of two-stage sintering schedules is of interest in its own right. Secondly, the work presented here provides a baseline for future work on the use of two-stage sintering processes for the fabrication of PMN–PFN composites.

2 Experimental Procedure

Two-stage mixed oxide routes[27] employing intermediate phases of $MgNb_2O_6$ and $FeNbO_4$ were adopted for the synthesis of PMN and PFN powders, respectively. Starting raw materials were reagent-grade PbO (>99·9%, Aldrich), $(MgCO_3)_4$ $Mg(OH)_2{\cdot}5H_2O$ (99%, Aldrich), Fe_2O_3 [99·5%, Alfa (Johnson Matthey)] and Nb_2O_5 (>99·9%, Alfa). The mixing process was carried out by vibro-milling the mixture of raw materials for 30 min with corundum media in isopropyl alcohol (IPA). After wet-milling, the slurry was dried, sieved, calcined, ground and sieved again to produce fine calcined powder. All powders were calcined in closed alu-

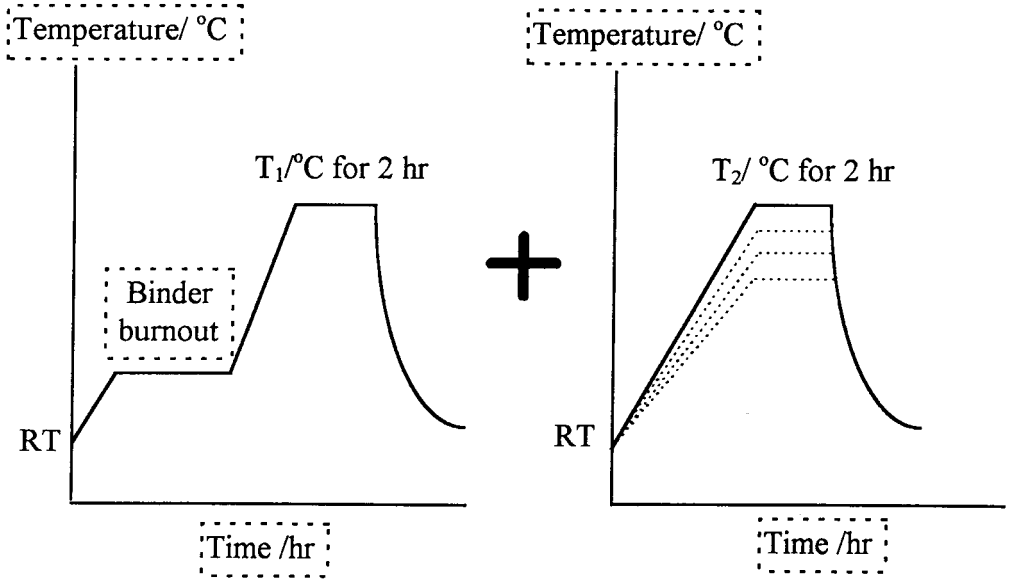

Fig. 1. Preparation of PMN and PFN ceramics employing a two-stage sintering method.

mina crucibles, with the optimum calcination temperatures determined by the XRD method [800°C with dwell-times of 4 h and 3 h for PMN and PFN, respectively (Fig. 1)].[27] Ceramic fabrication was carried out by adding 3 wt% polyvinyl alcohol (PVA) binder, prior to pressing as pellets in a pseudo-uniaxial die press at 100 MPa. Each pellet to be sintered was enclosed in a platinum foil and closed alumina crucible together with an atmosphere powder of identical chemical composition.[32,33] Sintering was carried out with a dwell-time of 2 h at each step, with constant heating rates of 10°C min^{-1} applied (Fig. 2). Two sets of the first sintering temperature (T_1) were investigated in each case: 1025°C and 1225°C for PMN; 925°C and 1125°C for PFN. Variation of the second sintering temperature (T_2) between 1050 and 1200°C and between 950 and 1100°C was carried out for PMN and PFN samples, respectively. Densities of the final sintered products were determined both by using the Archimedes principle and by geometrical measurement. XRD was used to examine the phases formed, with the microstructural features examined by scanning electron microscopy (SEM) equipped with an energy dispersive X-ray (EDX) analyser. Mean grain sizes of the sintered samples were subsequently estimated by employing the linear intercept method.

In order to evaluate the dielectric properties, densified samples were polished to form flat, parallel faces. Gold electrodes were applied to both surfaces by sputtering. Dielectric properties were measured at frequencies between 100 Hz and 100 kHz in the temperature range from +150 to −100°C, for a cooling rate of 0·5°C min^{-1}, using an HP4284A precision LCR meter in conjunction with a Delta Design 9023 temperature chamber.

3 Results and Discussion

3.1 Analysis of phases formed

X-ray diffraction patterns from the two sets of double-sintered PMN ceramics are given in Figs. 3 and 4, indicating the formation of both perovskite and pyrochlore phases in each case. The strongest reflections in the majority of the XRD patterns indicate the formation of the perovskite phase of lead magnesium niobate, $Pb(Mg_{1/3}Nb_{2/3})O_3$, which could be matched with JCPDS file 27-1199. A pseudo-cubic perovskite-type structure with cell parameter $a = 4{\cdot}049$ Å was identified. In this study, a single phase of perovskite PMN was found with two sets of sintering conditions: singly sintered at 1225°C [Fig. 4(a)] and doubly sintered at 1025°C/1100°C [Fig. 3(c)]. For the other sintering conditions, second phases were found to co-exist along with perovskite PMN. These correlate with two-types of pyrochlore phases, $Pb_3Nb_4O_{13}$ (marked by ▼) and $Pb_{1{\cdot}83}Nb_{1{\cdot}71}\ Mg_{0{\cdot}29}O_{6{\cdot}39}$ (marked by ▽), and could be matched with JCPDS files 25-443 and 37-71, respectively. The latter

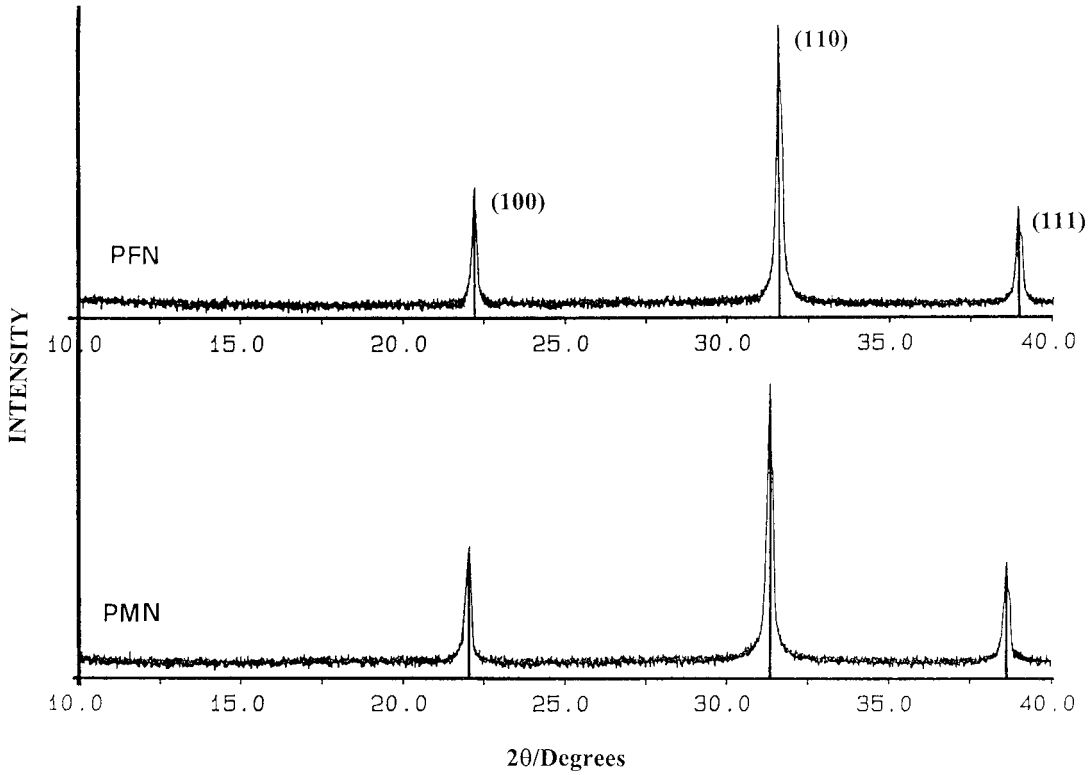

Fig. 2. XRD patterns of the starting precursors, calcined PMN and PFN powders.

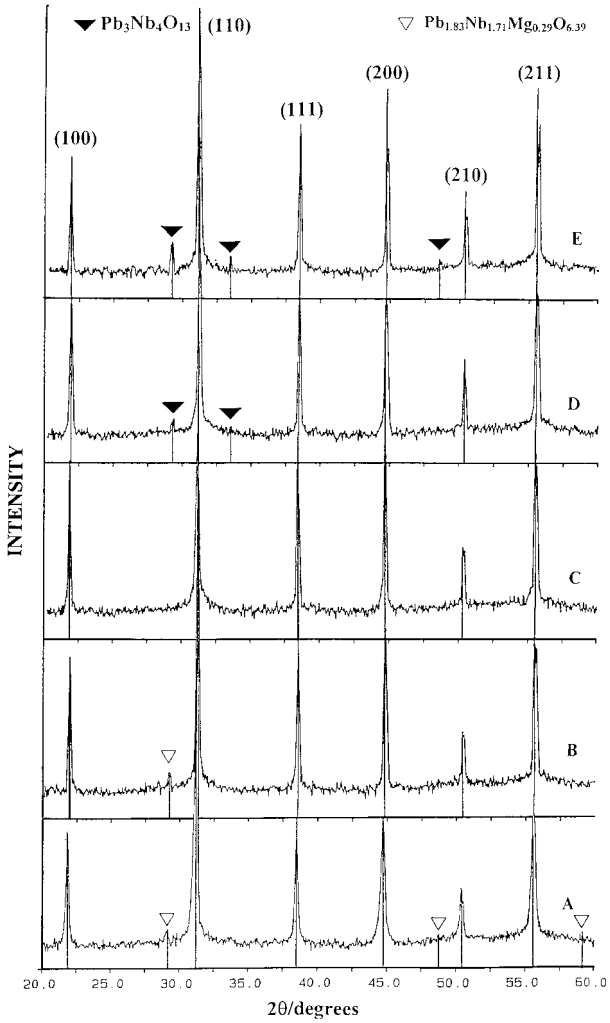

Fig. 3. XRD patterns of PMN ceramics sintered at (a) 1025°C, (b) 1025/1050°C, (c) 1025/1100°C, (d) 1025/1150°C and (e) 1025/1200°C, for constant dwell times of 2 h at each stage.

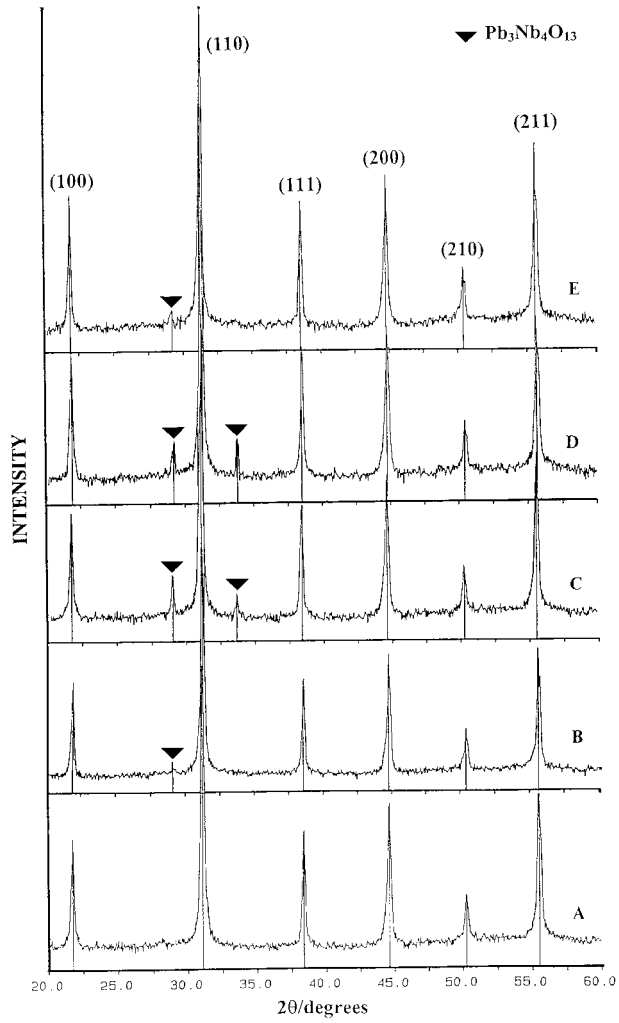

Fig. 4. XRD patterns of PMN ceramics sintered at (a) 1225°C, (b) 1225/1050°C, (c) 1225/1100°C, (d) 1225/1150°C and (e) 1225/1200°C, for constant dwell times of 2 h at each stage.

phase (▽) was detected in PMN samples which underwent lower temperature heat treatment at 1025°C [Fig. 3(a)] and double-sintering at 1025°C/1050°C [Fig. 3(b)].

XRD patterns from the two sets of doubly sintered PFN ceramics are given in Figs 5 and 6. The strongest reflections in the majority of the XRD traces indicate formation of the perovskite phase of lead iron niobate [$Pb(Fe_{1/2}Nb_{1/2})O_3$], with pseudocubic cell parameter $a = 4{\cdot}0148$ Å, which could be matched with JCPDS file 32-522. It is interesting to note that a single phase of perovskite is found in most of these doubly sintered PFN samples [Figs 5 (a), (d) and (e) and 6 (a), (b) and (e)], in contrast to the observations for PMN. Only small amounts of second phases could be detected by XRD, with additional reflections (marked by ▽), correlating with a pyrochlore phase of composition $PbFe_8O_{13}$ [JCPDS file 14-79; Figs 5 (b) and (c) and 6 (c) and (d)].

In order to evaluate the concentrations of perovskite and pyrochlore phases, the following approximation proposed by Swartz and Shrout[21] was employed (Tables 1 and 2): wt% perovskite phase

$$= \left(\frac{I_{\text{Perov}}}{I_{\text{Perov}} + I_{\text{Pyro}}}\right) + 100 \qquad (1)$$

Here I_{Perov} and I_{pyro} refer to the intensities of the perovskite {110} and pyrochlore peaks {222} for both $Pb_3Nb_4O_{13}$ and $Pb_{1{\cdot}83}Nb_{1{\cdot}71}Mg_{0{\cdot}29}O_{6{\cdot}39}$, and {201} for $PbFe_8O_{13}$, respectively, these being the most intense reflections of both phases.

It is seen in the tables that pyrochlore concentrations of up to about 4 wt% are estimated for doubly sintered PMN, these falling to less than 2 wt% for PFN. This could be due to the lower firing temperature of PFN compared to PMN, leading to a smaller degree of lead loss and a reduced tendency to form pyrochlore. However, many other factors come into play, e.g. homogeneity of materials, reactivity of starting powders, and processing variables.

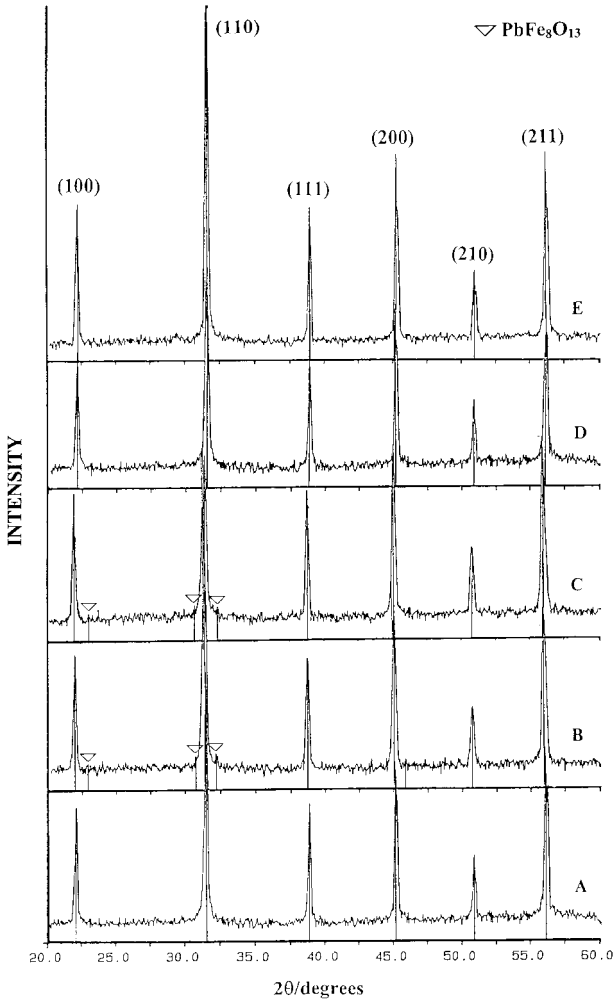

Fig. 5. XRD patterns of PFN ceramics sintered at (a) 925°C, (b) 925/950°C, (c) 925/1050°C, (d) 925/1100°C and (e) 925/1150°C, for constant dwell times of 2 h at each stage.

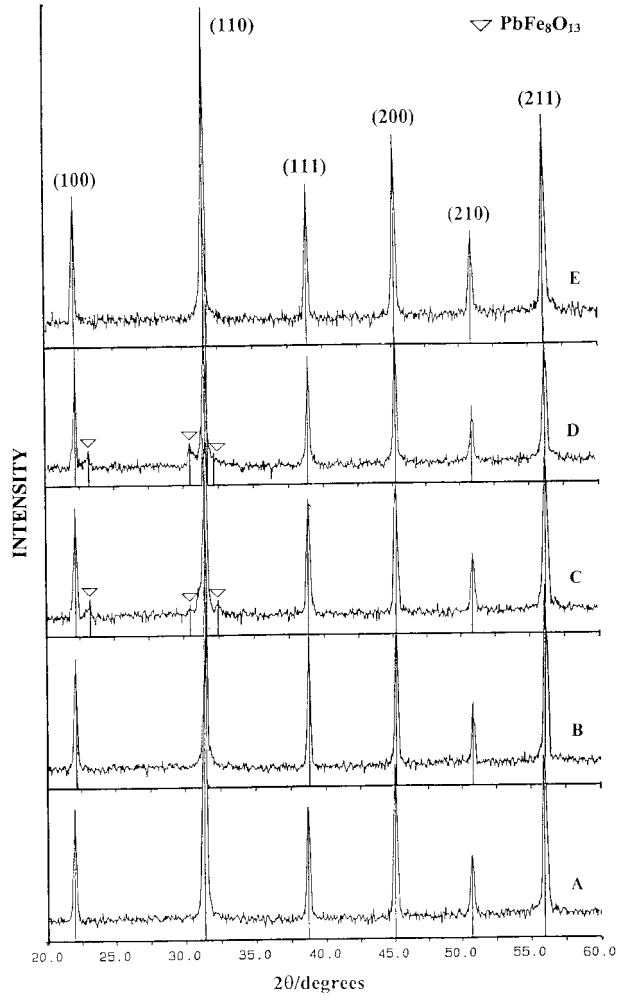

Fig. 6. XRD patterns of PFN ceramics sintered at (a) 1125°C, (b) 1125/950°C, (c) 1125/1000°C, (d) 1125/1050°C and (e) 1125/1100°C, for constant dwell times of 2 h at each stage.

3.2 Densification analysis

Weight losses upon sintering the PMN and PFN ceramics were calculated by recording the weights of the pellets before and after sintering. Densification characteristics, i.e. weight losses, calculated relative densities, concentrations of perovskite phase and mean grain sizes are summarised in Tables 1 and 2 for both systems. In general, there is a marked sensitivity of weight loss to the second sintering temperature, this increasing with temperature in both systems. However, by employing the atmosphere powder during the sintering process, the level of weight loss can be limited to less than 0·7% in both systems, in agreement with our earlier work on the conventional sintering of PMN and PFN.[32,33]

In general, low relative density values of less than 90% were obtained for most of the samples undergoing doubly sintering at low firing temperatures. For a given value of T_1, however, the observed bulk density value gradually increases with T_2. Relative densities could thus be obtained of 87–95 and 84–97% of the maximum values for PMN and PFN, respectively (Tables 1 and 2). Higher densities were obtained by raising T_2 further, i.e. to 1225°C in PMN and to 1125°C in PFN. The final densities obtained in both systems were thereby comparable with the results obtained by conventional sintering of PMN (1250°C for 2 h)[32] and PFN (1175°C for 2 h).[33] Thus the work here demonstrates that small reductions of ca 25°C in optimum sintering temperature may be obtained by the double-sintering technique, at the expense of longer firing cycles. Of more general importance, however, is the ability to match the densification obtained in a single-stage sintering process by a two-stage firing cycles, since the latter has been found to offers more versatility in the fabrication of PMN–PFN composites.

3.3 Microstructural analysis

Microstructural development during sintering was investigated by scanning electron microscopy (SEM) equipped with an EDX attachment. Micrographs of as-fired and fracture surfaces for some compositions in both PMN and PFN systems are

Table 1. Sintering behaviour on the two sets of doubly sintered PMN ceramics

T_1 (°C for 2 h)	T_2 (°C for 2 h)	Perovskite phase (wt%)	Weight loss (%)	Density (%)	Grain Size (μm)
1025	—	97·93	0·08	87	1–5
1025	1050	98·15	0·10	90	1–6
1025	1100	100	0·16	91	2–7
1025	1150	98·42	0·21	91	2–8
1025	1200	97·38	0·28	92	3–8
1225	1050	99·04	0·42	92	1–7
1225	1050	99·04	0·42	93	2–7
1225	1100	96·20	0·47	94	4–8
1225	1150	96·96	0·54	95	5–9
1225	1200	98·79	0·65	95	5–10

Table 2. Sintering behaviour on the two sets of doubly sintered PFN ceramics

T_1 (°C for 2 h)	T_2 (°C for 2 h)	Perovskite phase (wt%)	Weight loss (%)	Density (%)	Grain size (μm)
925	—	100	0·05	84	1–5
925	950	99·15	0·08	87	1–6
925	1000	99·38	0·10	88	2–8
925	1000	100	0·14	90	2–9
925	1100	100	0·21	91	1–10
1125	—	100	0·30	93	4–11
1125	950	100	0·42	95	4–12
1125	1000	99·05	0·45	96	4–14
1125	1050	98·35	0·51	97	6–18
1125	1100	100	0·63	97	7–20

shown in Figs. 7, 8(a)–(d) and 9, 10(a)–(d), respectively. These indicate the presence of both perovskite and pyrochlore phases. In general, the grains in all samples are similar in shape, with significant variations in size, particularly in samples sintered at low temperatures, which have a mean grain size in the range 1·0–5·0 mm. Higher T_2 values led to increases in grain-size (Table 1) and a more uniform microstructure, together with a greater tendency towards denser grain packing. Moreover, the grain shape tends towards greater sphericity at higher temperatures in both systems. The microstructural basis of the observed increase in relative density with sintering cycle is apparent from progressively enhanced grain packing, along with changes in morphology of the fracture surfaces. Pyrochlore-type phases can be found in these SEM micrographs, in particular at the grain boundaries and at the triple point junctions. These phases can be clearly distinguished from the microstructural features of the perovskite parent phase, in terms of both brightness (too bright or too dark) and shape (mostly octahedral or rectangular in shape). Energy dispersive X-ray (EDX) analysis showed the chemical compositions of these pyrochlore phases to be $Pb_3Nb_4O_{13}$, in agreement with XRD results.

Microstructural features of PMN samples sintered at 1025, 1025/1100 and 1025/1200°C (for dwell-time of 2 h at each stage), are shown in Fig. 7(a), (b) and (c), respectively. In Fig. 7(a), a uniform grain shape is observed, with sizes in the range between 1·0 and 5·0 μm for the parent PMN phase, in which some pyrochlore particles are also found. The rectangular shape ($\sim$ 1·0 μm) of the $Pb_3Nb_4O_{13}$ pyrochlore phase is observed (at the centre of the white square) at the grain boundaries of the parent phase. In samples subjected to higher temperatures, this pyrochlore phase cannot be found [Fig. 7 (b) and (c)], whereas another type of pyrochlore phase $Pb_{1·83}Nb_{1·71}Mg_{0·29}O_{6·39}$ with an octahedral morphology is observed, somewhat surprisingly, over the as-fired surface of the PMN sample sintered at 1025°C/1200°C [Fig. 7 (c) and (d)]. Grain sizes within the approximate range of 5·0–6·5 μm could be determined for this pyrochlore $Pb_{1·83}Nb_{1·71}Mg_{0·29}O_{6·3}$, whilst the grain size of the parent phase is in the range of 3·5–8·0 μm. Moreover, it is seen that there are some MgO inclusions (brighter phase with a small spherical shape; diameter ca 1·0–2·0 μm) existing alongside this pyrochlore phase. These two phases of $Pb_{1·83}Nb_{1·71}Mg_{0·29}O_{6·3}$ and MgO are consistent with the minor phases commonly found in the preparation of PMN.[15,19,29,30] The existence of a discrete MgO phase points to the poor reactivity of PbO and MgO, although the concentration is too low for detection by XRD.

Representative microstructures for doubly sintered PMN ceramics with $T_2 = 1225$°C are given in Fig. 8(a), (b) and (c), respectively. Here, pyrochlore

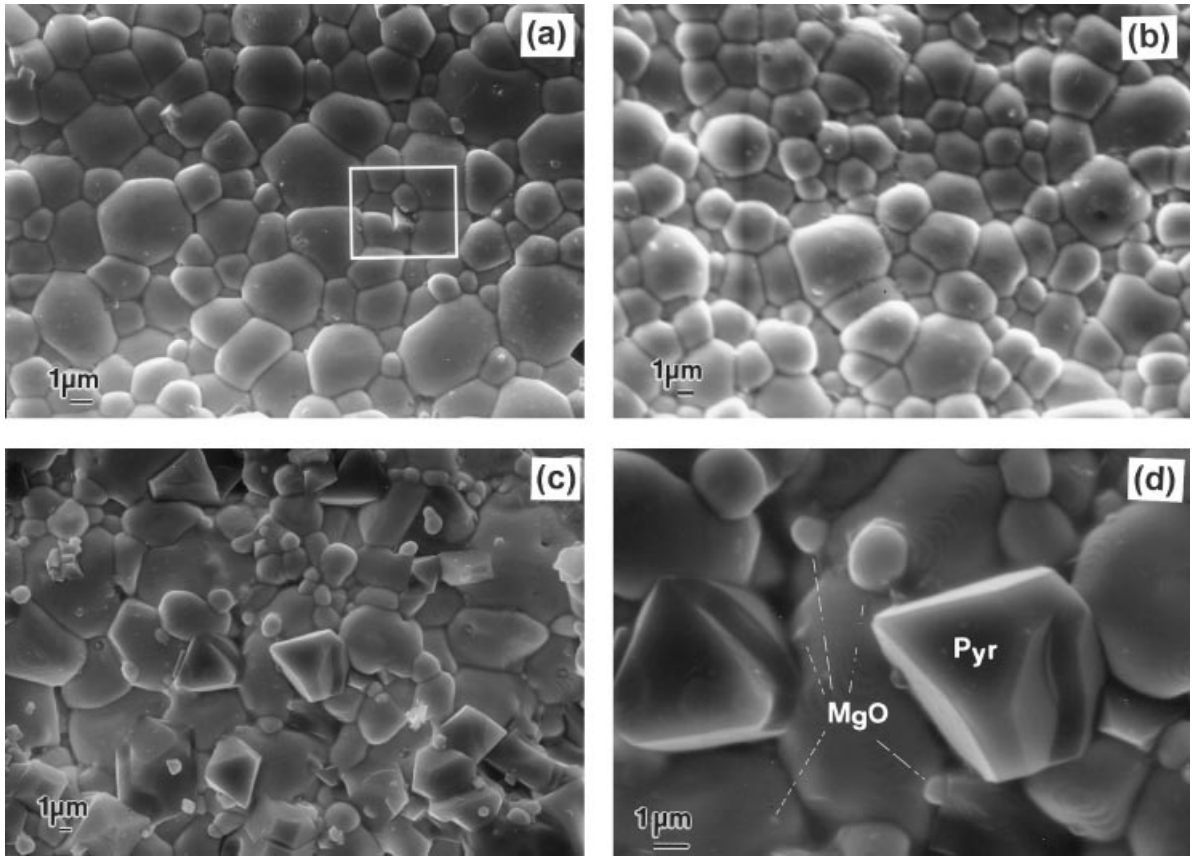

Fig. 7. SEM micrographs of as-fired surface of PMN ceramics sintered at (a) 1025°C, (b) 1025/1100°C, (c) and (d) 1025/1200°C, for constant dwell times of 2 h at each stage.

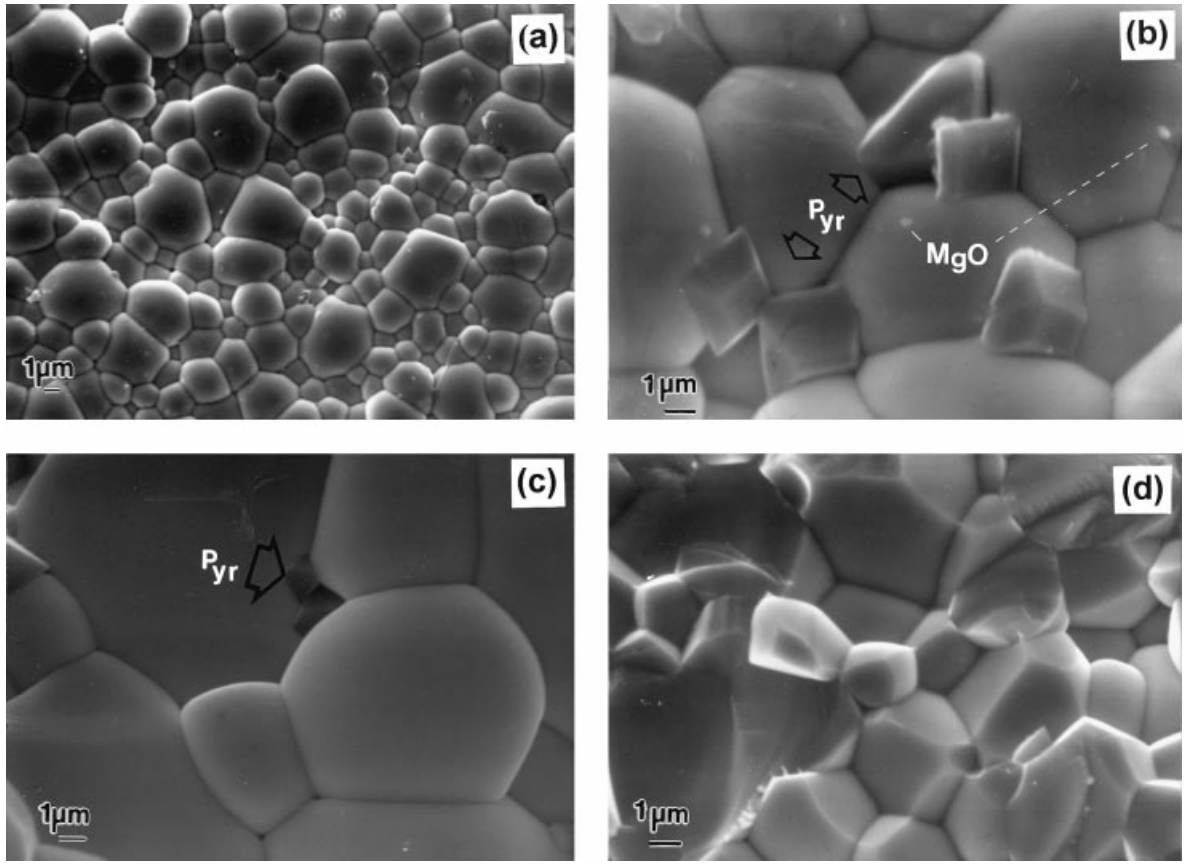

Fig. 8. SEM micrographs of as-fired surface of PMN ceramics sintered at (a) 1225°C, (b) 1225/1100°C, (c) 1225/1200°C and (d) fracture surface of PMN ceramics sintered at 1225/1200°C, for constant dwell times of 2 h at each stage.

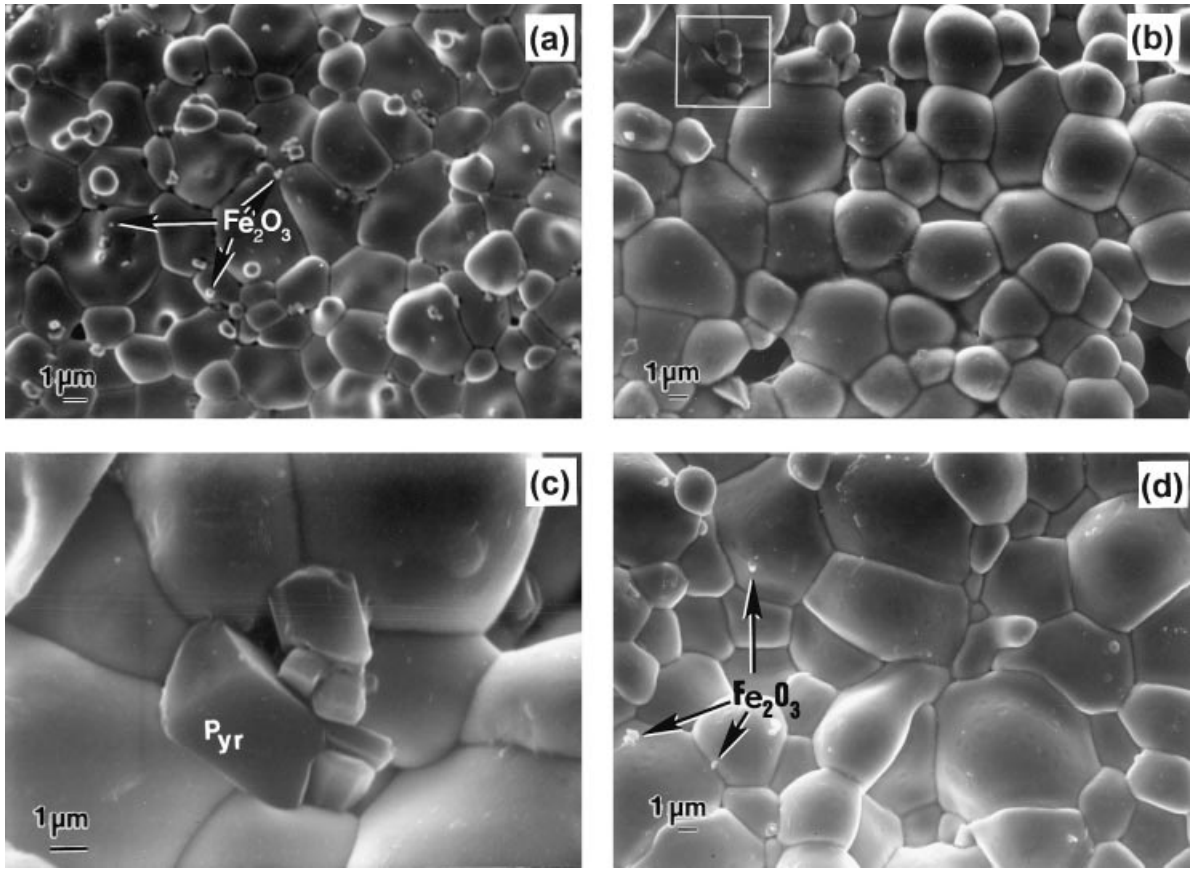

Fig. 9. SEM micrographs of as-fired surfaces of PFN ceramics sintered at (a) 925°C, (b) 925/1000°C, (c) higher magnification of (b), and (d) 925/1100°C, for constant dwell times of 2 h at each stage.

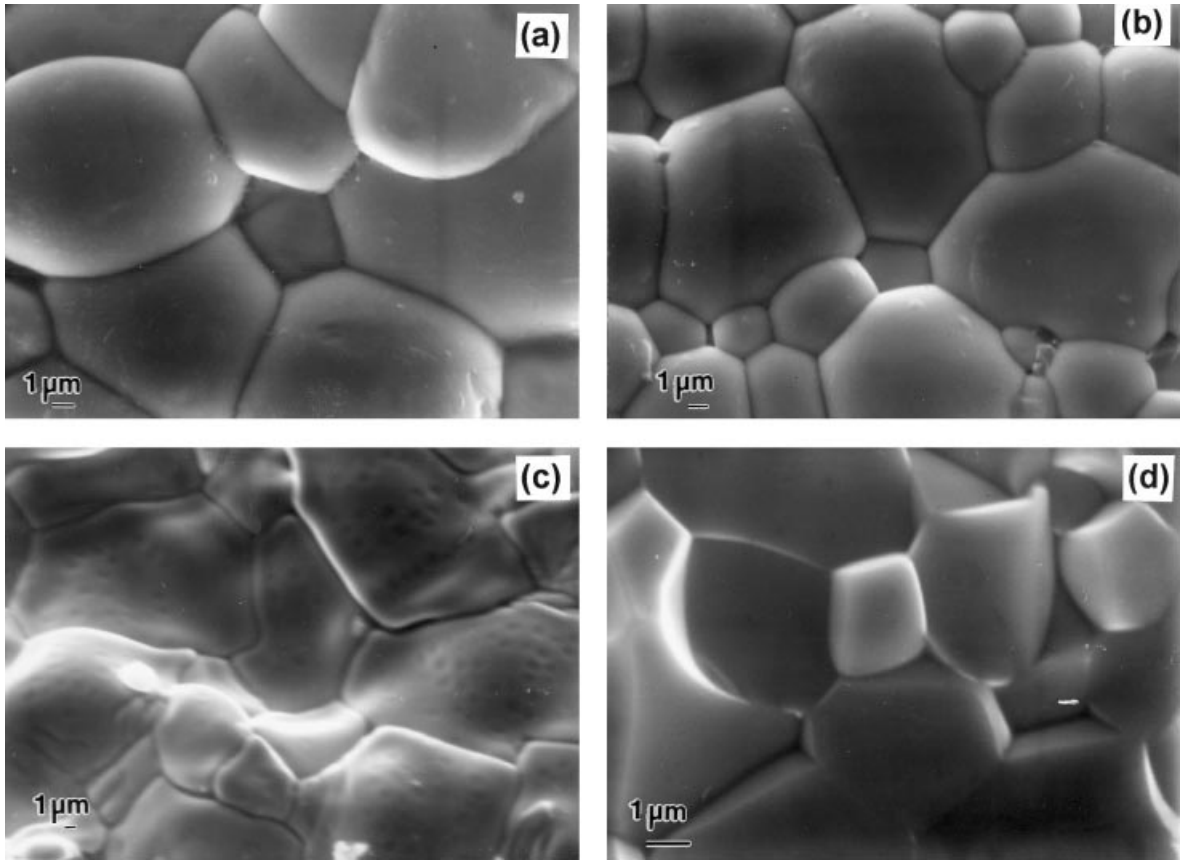

Fig. 10. SEM micrographs of as-fired surfaces of PFN ceramics sintered at (a) 1125°C, (b) 1125/1000°C, (c) 1125/1100°C and (d) fracture surfaces of PFN ceramics sintered at 1125/1100°C, for constant dwell times of 2 h at each stage.

phases of composition $Pb_{1.83}Nb_{1.71}Mg_{0.29}O_{6.39}$ (octahedral shape) are found, with particle sizes of about 3·0 to 5·0 μm, located at both triple junction and grain boundaries. Evidence of MgO inclusions is also found.

Indicative microstructures obtained for PFN under corresponding conditions are given in Figs. 9 and 10 for T_2-values of 1100 and 1200°C. By comparison with PMN samples, the microstructures of PFN samples are generally found to exhibit slightly denser angular grain-packing with a uniform grain size. A distribution of very small spherical Fe_2O_3 inclusions (more brightly shaded), over the PFN grains, is also found, by analogy with MgO inclusions in PMN. Moreover, agglomerated pyrochlore phases of $PbFe_8O_{13}$ with highly angular grains are observed at triple points of the parent PFN phase, when sintered at 925°C/1100 [Fig. 9(b)]. This microstructural feature is also found in Fig. 9(c), at higher magnification. A grain size of approximately 5·0–7·0 μm was determined for this pyrochlore phase.

Typical microstructures of PFN sintered at 1125, 1125/1100°C and 1125/1200°C are shown in Fig. 10(a), (b) and (c), respectively. It is seen that, for higher temperature treatments, almost clean microstructures with highly uniform, dense grain packing are generally found. Only small amounts of spherical grains of Fe_2O_3 are

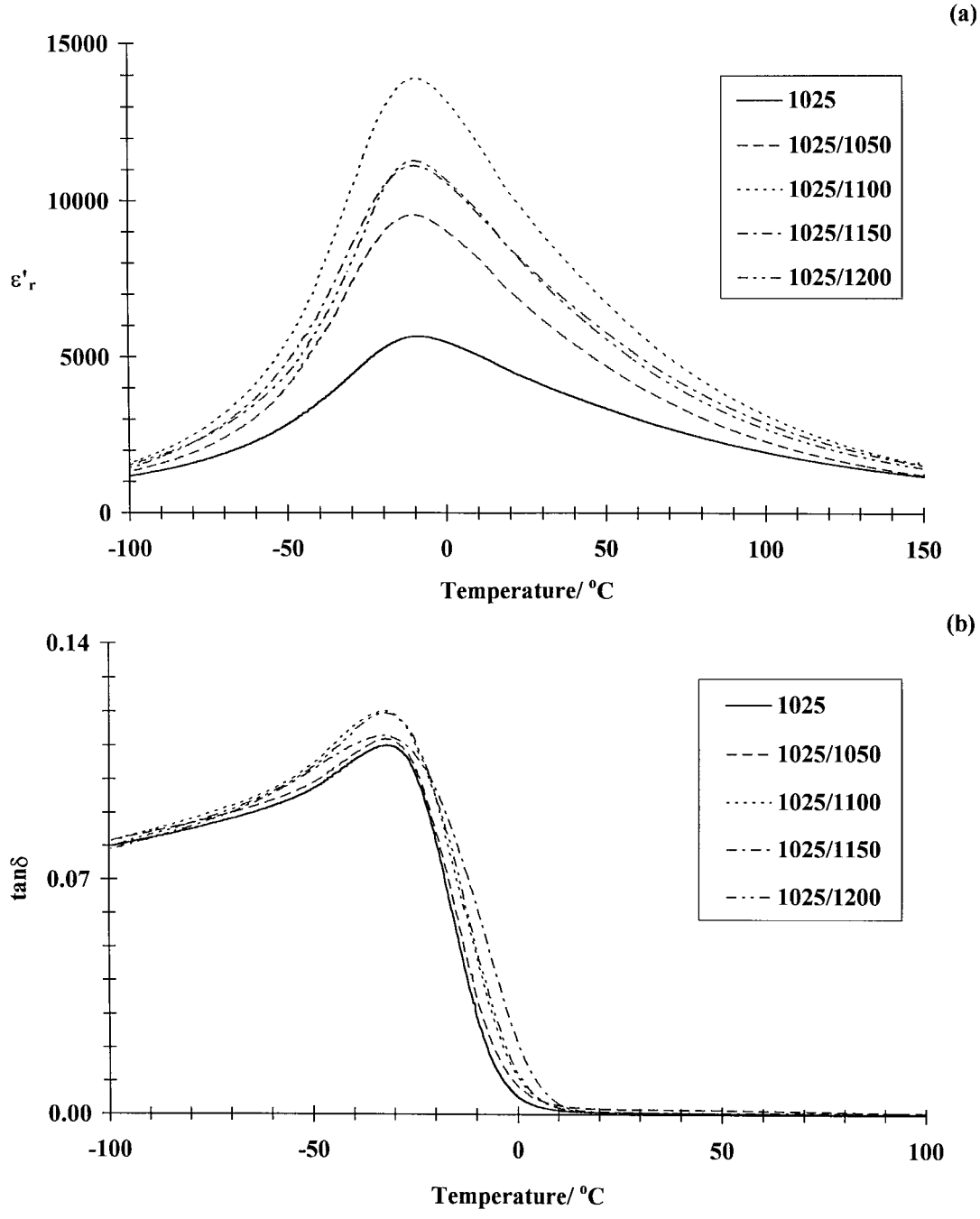

Fig. 11. Variation with temperature of (a) relative permittivity and (b) dissipation factor at 1 kHz for PMN ceramics sintered at $T_1 = 1025$°C for 2 h and varying T_2 from 1000°C to 1200°C for constant dwell times of 2 h.

observed. No significant amounts of pyrochlore phase could be found in this system. It is interesting to note that highly dense grain-packing with thinner grain boundaries is observed in PFN sintered at 1125°C/1200°C, Fig. 10(c), which is consistent with the dense grain packing found in fracture surfaces [Fig. 10(d)].

In general, the pyrochlore phases identified in both systems by SEM/EDX are in agreement with XRD results. However the advantage of SEM here lies in its ability to reveal microstructural features often missed by X-ray diffraction, such as MgO and Fe_2O_3 inclusions.

3.4 Dielectric response of the ceramics

The temperature dependences of (a) relative permittivity (ε'_r) and (b) dissipation factor (tanδ) at 1 kHz are shown in Fig. 11–14 for the two sets of doubly sintered PMN and PFN ceramics, respectively. The values of $\varepsilon'_{r,\max}$, $\tan\delta_{\max}$ and temperatures $T(\varepsilon'_{r,\max})$ and $T(\tan\delta_{\max})$ obtained under different sintering conditions for the two sets of doubly sintered PMN and PFN are given in Tables 3 and 4, respectively. Sintered PMN ceramics exhibit typical relaxor ferroelectric responses, with temperatures of maximum permittivity, $T(\varepsilon_{r,\max})$, of about -10°C. By comparison, the sintered PFN ceramics represent

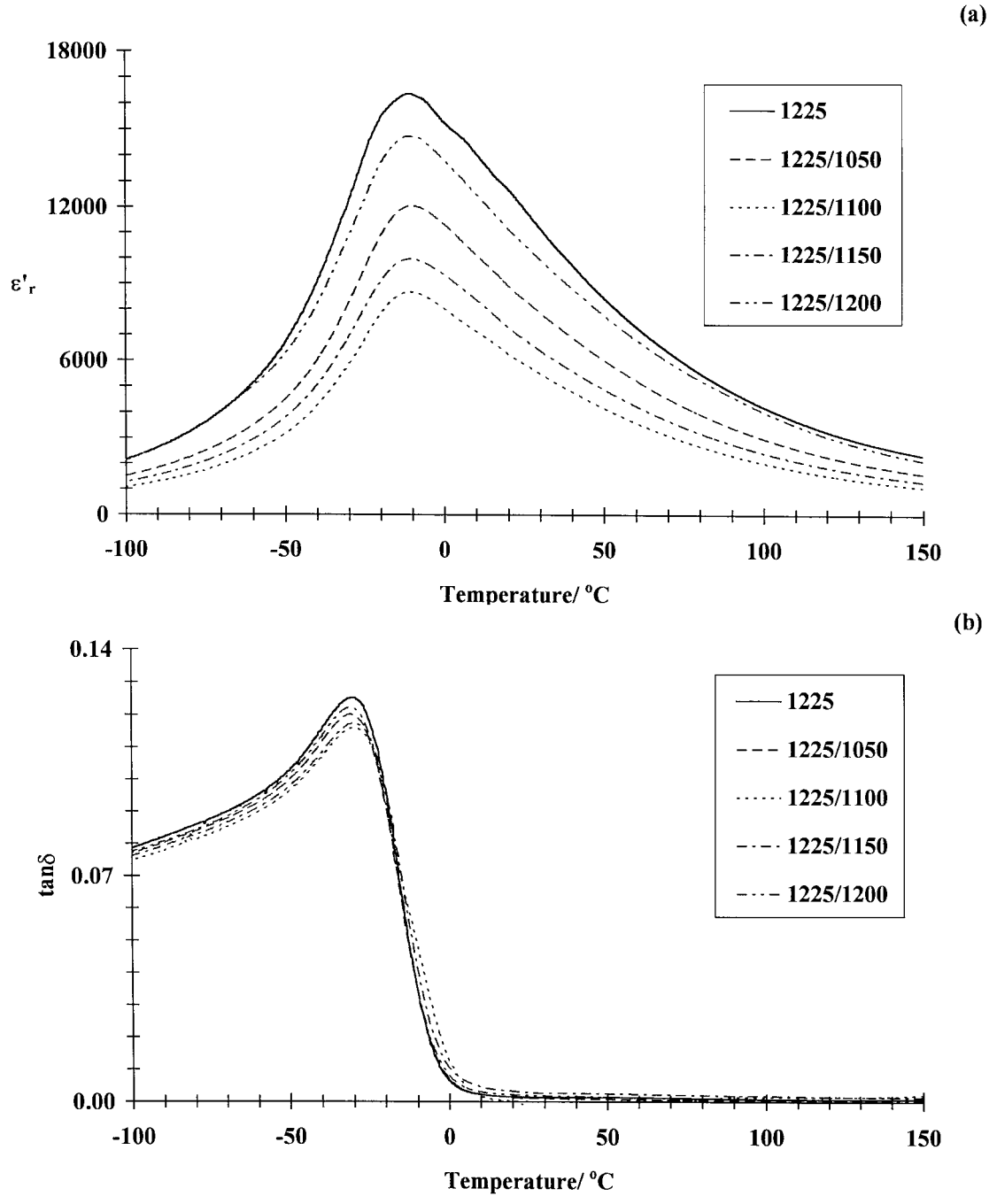

Fig. 12. Variation with temperature of (a) relative permittivity and (b) dissipation factor at 1 kHz for PMN ceramics sintered at $T_1 = 1225$°C for 2 h and varying T_2 from 1000°C to 1200°C for constant dwell times of 2 h.

nearly normal ferroelectric behaviour (i.e. a sharper relative permittivity response with reduced frequency dispersion) with higher $T(\varepsilon_{r,\max})$-values of 110°C, in agreement with earlier work.[3,15,34] Here, it is found that the magnitudes of both $\varepsilon'_{r,\max}$ and $\tan\delta_{\max}$ in sintered PMN and PFN samples depend considerably upon the heat treatment conditions.

In Fig. 11(a), the $\varepsilon_{r,\max}$-value of PMN (for $T_1 = 1025$°C) increases from 5500 to 14000 as T_2 rises from 1050 to 1100°C, then sharply decreases to 11000 at $T_2 = 1150$°C. This value is retained for further increases of T_2 up to 1200°C. On the other hand, in the PMN system [$T_1 = 1225$°C; Fig. 12(a)], it is seen that the $\varepsilon_{r,\max}$-value decreases markedly from 16 500 to 8500, as T_2 rises from 1050 to 1100°C. Upon further increases of T_2 up to 1200°C, $\varepsilon_{r,\max}$ rises significantly to about 14 500. This trend is opposite to that observed for the lower T_1-value.

From the results in Sections 3·1 and 3·2, it follows that the dielectric response of PMN ceramics is remarkably sensitive both to pyrochlore formation and to the densification of the final ceramics. Poor

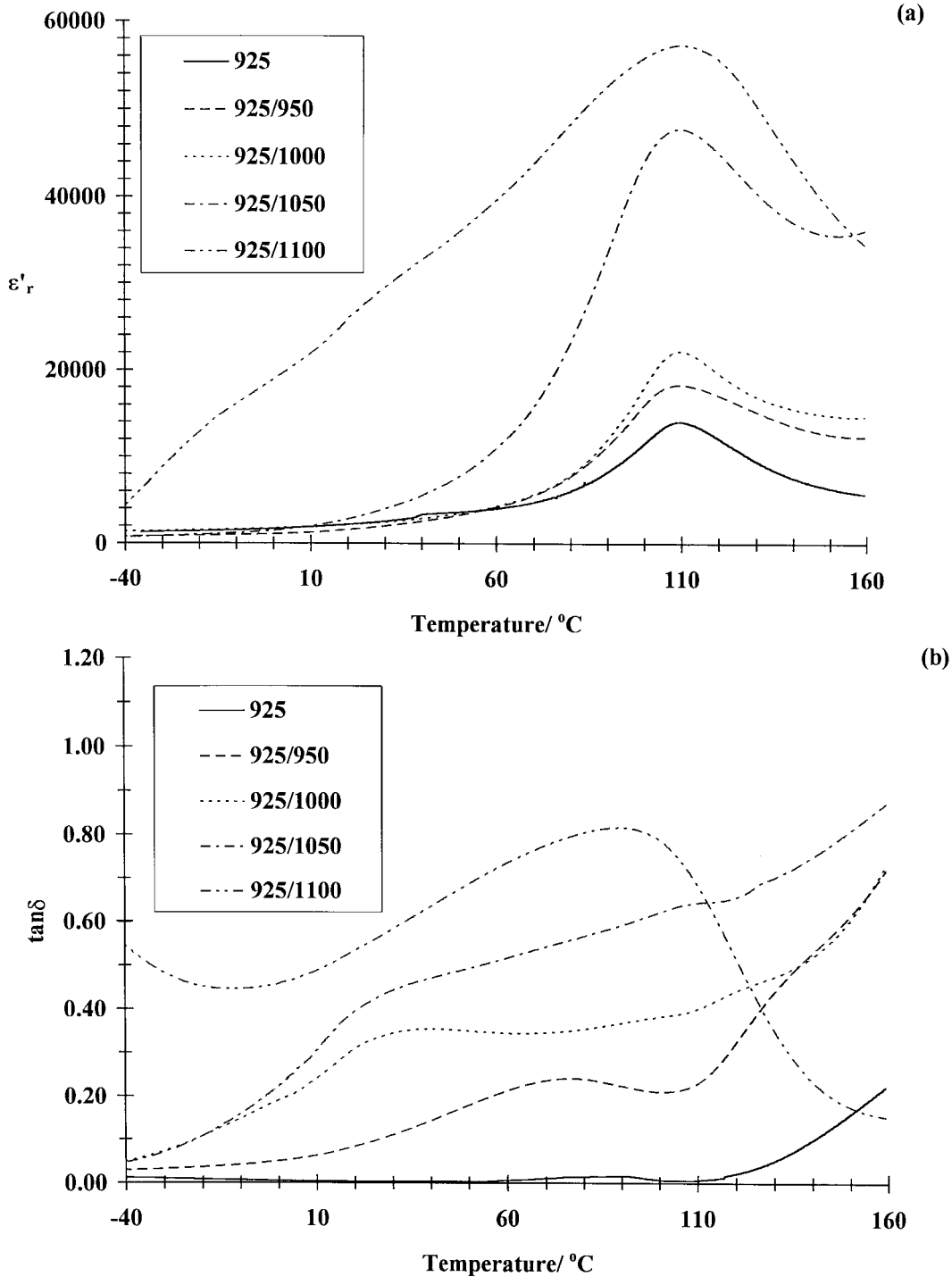

Fig. 13. Variation with temperature of (a) relative permittivity and (b) dissipation factor at 1 kHz for PFN ceramics sintered at $T_1 = 925$°C for 2 h and varying T_2 from 950°C to 1100°C for constant dwell times of 2 h.

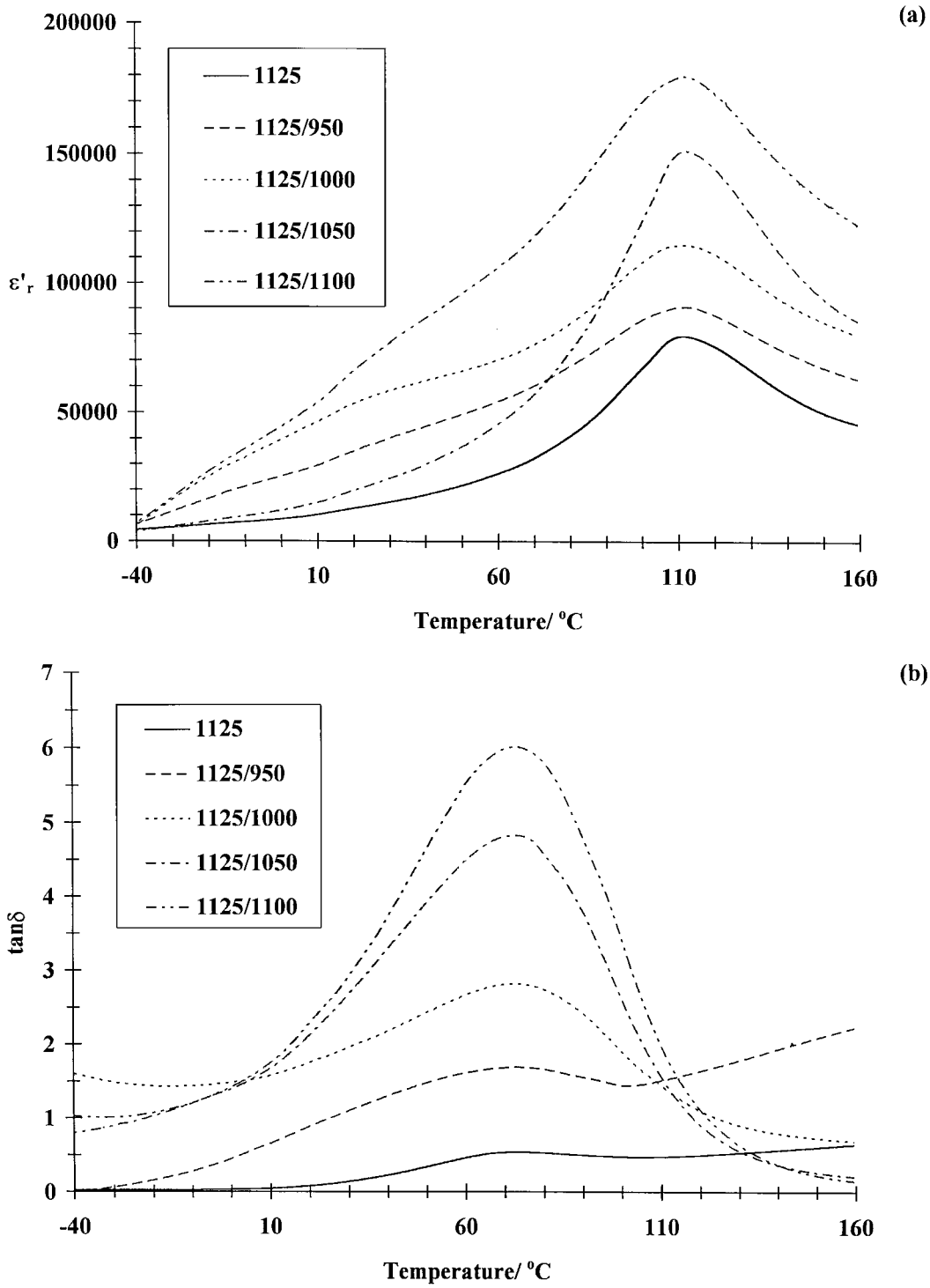

Fig. 14. Variation with temperature of (a) relative permittivity and (b) dissipation factor at 1 kHz for PFN ceramics sintered at $T_1 = 1125°C$ for 2 h and varying T_2 from 950°C to 1100°C for constant dwell times of 2 h.

dielectric properties are observed in low density PMN samples with high pyrochlore contents. Owing to the low relative permittivity values of these paraelectric pyrochlore phases at room temperature, i.e. $\varepsilon'_r \sim 130$ for $Pb_{1.83}Nb_{1.71}Mg_{0.29}O_{6.3}$ pyrochlore,[12], the potential effect on the relative permittivity of the final product is very significant. Small amounts occurring as discrete particles have less effect than pores of corresponding volume, but they may considerably reduce the permittivity if present as an intergranular phases, thereby interposing low ε'_r regions between grains of the high ε'_r phase, i.e. PMN or PFN. Larger amounts will result in significant compositional changes of the perovskite-type phases.

The variation of $\tan\delta_{max}$ with sintering conditions in doubly sintered PMN is analogous to that of $\varepsilon'_{r,max}$, but not as marked [Figs. 11(b) and 12(b)]. The level of frequency dispersion is given by the parameters $\Delta T' = T(\varepsilon'_{r,max})100kHz - T(\varepsilon'_{r,max})100Hz$, and $\Delta T'' = T(\varepsilon''_{r,max})100kHz - T(\varepsilon''_{r,max})100Hz$ as previously employed.[5,6,15,18]

Table 3. Dielectric properties at 1 kHz of the two stes of doubly sintered PMN ceramics

T_1 (°C for 2 h)	T_2 (°C for 2 h)	$\varepsilon'_{r,max}$	$T(\varepsilon'_{r,max})$ (°C)	$\Delta T'$ (K)	$tan\delta_{max}$	$T(tan\delta_{max})$ (°C)	$\Delta T''$ (k)
1025	—	5658	−10	17	0·1102	−31	15
1025	1025	9553	−10	17	0·1121	−31	15
1025	1100	13910	−10	17	0·1203	−31	15
1025	1150	11150	−10	16	0·1130	−31	16
1050	1200	11310	−10	17	0·1197	−31	16
1225	—	16358	−10	16	0·1252	−31	14
1225	1050	12050	−10	17	0·1201	−31	14
1225	1100	8667	−10	16	0·1159	−31	14
1225	1150	9959	−10	16	0·1173	−31	15
1225	1200	14750	−10	17	0·1222	−31	15

Table 4. Dielectric properties at 1 kHz of the two sets of doubly sintered PFN ceramics

T_1 (°C for 2 h)	T_2 (°C for 2 h)	$\varepsilon'_{r,max}$	$T(\varepsilon'_{r,max})$ (°C)	$\Delta T'$ (K)	$tan\delta_{max}$	$T(tan\delta_{max})$ (°C)	$\Delta T''$ (k)
925	—	14 029	110	0	0·0154	80	5
925	950	18 260	110	1	0·2401	76	7
925	1000	22 140	110	1	0·3533	45	9
925	1050	47 770	110	1	—	—	—
925	1100	57 270	110	1	0·8170	86	9
1125	—	79 490	110	1	0·5357	72	10
1125	950	90 910	110	0	1·6850	72	12
1125	1000	115 122	110	1	2·8230	72	7
1125	1050	151 500	110	0	4·8280	72	8
1125	1100	179 800	110	0	6·0114	73	7

From Tables 3 and 4, it is seen that values of 16–17 and 14–15 are obtained for $\Delta T'$ and $\Delta T''$, respectively.

The effects of varying T_1 and T_2 on the dielectric response of PFN ceramics differ from the PMN system. $\varepsilon'_{r,\max}$ values gradually increase with T_2, for both T_1-values [Figs. 13 (a) and 14 (a)]. Furthermore, it is interesting to note that the magnitude of $\varepsilon'_{r,\max}$, value of up to 180 000 at 1 kHz ($T_1 = 1125$°C; $T_2 = 1100$°C) is higher than the maximum value observed in our earlier work on PFN normally sintered at 1175°C.[31] However, an extremely high dissipation factor of tanδ ~6·0 is observed in this sample. As previously observed[33] with PFN ceramics, particularly in samples sintered at high temperatures, high values of both relative permittivity and dissipation factor point to the conductivity effects related to Fe^{2+}/Fe^{3+} electron-hopping.[33]

In the present work, the value of tanδ is too high for general device utilisation. Therefore, further work is required to reduce the dissipation factor of PFN to an acceptable level, probably by employing some additive e.g. lithium or manganese,[36] along with an exploration of hot isostatic pressing techniques. The variation of $\tan\delta_{\max}$ with sintering conditions in doubly sintered PFN also follows that of $\varepsilon'_{r,\max}$ [Figs. 13 (b) and 14 (b)]. From Table 4, it is seen that a value approaching zero could be obtained for $\Delta T'$, in agreement with other work.[34]

Although a disadvantage of the proposed two-stage sintering method is a greater time-requirement, the small reduction in firing temperature is a positive development, particularly with regard to the drive towards electrodes of lower cost. Further work on the effects of varying sintering conditions would be of benefit. In particular, an optimised two-stage sintering technique might find application in other lead-based relaxor perovskite systems, e.g. PZN, PMNT, PFW, along with other systems employing oxides with lower melting points. The two-stage sintering technique also forms the baseline for further work on the manufacturing of PMN–PFN composites.[37]

4 Conclusion

The potential of a two-stage sintering method has been investigated for the production of PMN and PFN ceramics for dielectric applications. It has been shown that, under suitable conditions, the properties of the ceramics may be equivalent to those obtained from a single sintering stage. Three aspects of this work are significant: (i) small reductions in the maximum required sintering temperature are possible compared to single-stage sintering; (ii) new insight into the dependence of dielectric properties on microstructure and the formation of second phases has been obtained; (iii) a

framework has been established for developing two-stage sintering methods for the manufacture of PMN–PFN composites.

Acknowledgements

One of the authors (S.A.) wishes to thanks the DPST project and the Thai Government for financial support during his study.

References

1. Okazaki, K., Advanced technology in electroceramics in Japan. *Am. Ceram. Soc. Bull*., 1988, **67**(12), 1946–1960.
2. Uchino, K., Electrostrictive actuators: materials and Applications. *Am. Ceram. Soc. Bull*, 1986, **65**, 647–652.
3. Shrout, T. R. and Halliyal, A., Preparation of lead-based ferroelectric relaxor for capacitors. *Am. Ceram. Soc. Bull*., 1987, **66**, 704–711.
4. Beck, C. M., Thomas, N. W. and Thompson, I., Cobalt-doping of lead magneisum niobium titanate: chemical control of dielectric properties. *J. Eur. Ceram. Soc*., 1998, **18**, 1679–1684.
5. Beck, C. M., Thomas, N. W. and Thompson, I., Manganese-doping of lead magneisum niobium titanate: chemical control of dielectric properties. *J. Eur. Ceram. Soc*, 1998, **18**, 1685–1693.
6. Imoto, F. and Ilda, H., The formation process of lead magnesio-niobate in the solid state reaction. *J. Ceram. Soc. Jap*, 1972, **80**, 25–31.
7. Kassarjian, M. P., Newnham, R. E. and Biggers, J. V., Sequence of reactions during calcining of lead-iron niobate dielectric ceramics. *Am. Ceram. Soc. Bull*., 1985, **64**, 1111–1180.
8. Nomura, S., Kuwata, J., Jang, S. J., Cross, L. E. and Newnham, R. E., Electrostriction in $Pb(Zn_{1/3}Nb_{2/3})O_3$. *Mater. Res. Bull*., 1979, **14**, 769–774.
9. Mizutani, N., Lu, C. H., Shinozaki, K. and Kato, M., Formation of a high-temperature liquid phase during the sintering of $Pb(Fe_{2/3}W_{1/3})O_3$. *J. Am. Ceram. Soc*., 1990, **73**, 1214–1220.
10. Yokosuka, M., Electrical and Electromechanical Properties of Hot-Pressed $Pb(Fe_{1/2}Nb_{1/2})O_3$ Ferroelectric Ceramics. *Jpn. J. Appl. Phys. Part1*, 1993, **32**, 1142–1146.
11. Lejeune, M. and Boilot, J. P., Formation mechanism and ceramic process of the ferroelectric perovskites: $Pb(Mg_{1/3}Nb_{2/3})O_3$ and $Pb(Fe_{1/2}Nb_{1/2})O_3$. *Ceram. Inter*., 1982, **8**, 99–103.
12. Shrout, T. R. and Swartz, S. L., Dielectric properties of pyrochlore lead magnesium niobate. *Mater. Res. Bull*., 1983, **18**, 663–667.
13. Dambekalne, M., Brante, I. and Sternberg, A., The formation process of complex lead-containing niobates. *Ferroelectrics*, 1989, **90**, 1–14.
14. Chaput, F., Boilot, J. P., Lejeune, M., Papiernik, R. and Hubert-Pfalzgraf, L. G., Low-temperature route to lead magnesium niobate. *J. Am. Ceram. Soc*., 1989, **72**, 1355–1357.
15. Chen, J. and Harmer, M. P., Microstructure and dielectric properties of lead magnesium niobate-pyrochlore diphasic mixtures. *J. Am. Ceram. Soc*., 1990, **73**, 68–73.
16. Ling, H. C., Yan, M. F., Jackson, A. M. and Rhodes, W. W., Effect of PbO evaporation on the composition and dielectric properties of $PbO\text{-}MgO\text{-}Nb_2O_5$ based dielectrics. *J. Mater. Res*, 1990, **5**, 629–639.
17. Wakiya, N., Saiki, A., Ishizawa, N., Shinozaki, K. and Mizutani, N., Crystal growth, crystal structure and chemical composition of pyrochlore type compound in lead-magnesium-niobium-oxygen system. *Mat. Res. Bull*, 1993, **28**, 137–143.
18. Wakiya, N., Kim, B. H., Shinozaki, K. and Mizutani, N., Composition range of cubic pyrochlore type compound in lead-magnesium-niobium-oxygen system. *J. Ceram. Soc. Jap*., 1994, **102**, 612–615.
19. Mergen, A. and Lee, W. E., Fabrication, characterisation and formation mechanism of $Pb_{1.83}Mg_{0.29}Nb_{1.71}O_{6.39}$ pyrochlore. *J. Eur. Ceram Soc*, 1997, **17**, 1033–1047.
20. Mergen, A., Reaney, I. M. and Lee, W. E., Microstructures of pyrochlore-perovskite mixtures in $PbO\text{-}MgO\text{-}Nb_2O_5$ system. *Brit. Ceram. Trans*, 1997, **96**, 41–49.
21. Swartz, S. L. and Shrout, T. R., Fabrication of perovskite lead magnesium niobate. *Mat. Res. Bull*, 1982, **17**, 1245–1250.
22. Guha, J. P. and Anderson, H. U., Preparation of perovskite $Pb(Mg_{1/3}Nb_{2/3})O_3$ using $Pb_3Nb_2O_8$ and MgO. *J. Am. Ceram. Soc*, 1986, **69**, 287–288.
23. Lejeune, M. and Boilot, J. P., Influence of ceramic processing on dielectric properties of perovskite type compound: $Pb(Mg_{1/3}Nb_{2/3})O_3$. *Ceram. Inter*., 1983, **9**, 119–122.
24. Chen, J., Gorton, A., Chan, H. M. and Harmer, M. P., Effect of powder purity and second phases on the dielectric properties of lead magnesium niobate ceramics. *J. Am. Ceram. Soc*., 1986, **69**, 303–305.
25. Fu, S. L. and Chen, C. F., Fabrication of perovskite $Pb(Fe_{1/2}Nb_{1/2})O_3$ and reaction mechanism. *Ferroelectrics*, 1989, **82**, 119–126.
26. Butcher, S. J. and Daglish, M., The use of magnesium carbonate hydroxide pentahydrate in the production of perovskite lead magnesium niobate. In *Third Euro-eramics Conference Proceedings*, ed. P. Duran and J. F. Fernandez. ERSC, Spain, 1993, pp. 121–126.
27. Ananta, S. and Thomas, N. W., A modified two-stage mixed oxide synthetic route to lead magnesium niobate and lead iron niobate. *J. Eur. Ceram. Soc*., 1999, **19**(2), 155–163.
28. Vilarinho, P. M. and Baptista, J. L., Effect of excess of iron oxide and lead oxide on the microstructure and dielectric properties of lead-iron tungstate ceramics. *J. Eur. Ceram. Soc*, 1993, **11**, 407–415.
29. Wang, H. C. and Schulze, W. A., The role of excess magnesium oxide or lead oxide in determining the microstructure and properties of lead magnesium niobate. *J. Am. Ceram. Soc*, 1990, **73**, 825–832.
30. Goo, E., Yamamoto, T. and Okazaki, K., microstructure of lead–magnesium niobate ceramics. *J. Am. Ceram. Soc*., 1986, **69**, 188–190.
31. Sekar, M. M. A., Halliyal, A. and Patil, K. C., Synthesis, characterisation, and properties of lead-based relaxor ferroelectrics. *J. Mater. Res*., 1996, **11**, 1210–1218.
32. Ananta, S. and Thomas, N. W., Relationships between sintering conditions, microstructure and dielectric properties of lead magnesium niobate. *J. Eur. Ceram. Soc*., 1999, **19**(5), 629–635.
33. Ananta, S. and Thomas, N. W., Fabrication and characterisation of PFN ceramics. *J. Eur. Ceram. Soc*., in press.
34. Chiu, C. C. and Desu, S. B., Microstructure and properties of lead ferroelectric ceramics ($Pb(Fe_{0.5}Nb_{0.5})O_3$). *Mat. Sci. Eng*., 1993, **B21**, 26–35.
35. Lejeune, M. and Boilot, J. P., Optimization of dielectric properties of lead–magnesium niobate ceramics. *Am. Ceram. Soc. Bull*, 1985, **64**, 679–682.
36. Kassarjian, M. P., Newnham, R. E. and Biggers, J. V., Reduction of losses in lead–iron niobate dielectric ceramics. *Am. Ceram. Soc. Bull*, 1985, **64**, 1245–1248.
37. Ananta, S. and Thomas, N.W., Mixed-sintering of PMN–PFN ceramic–ceramic composites. *J. Eur. Ceram. Soc*. in preparation.